Journal of Cardiology 61 (2013) 149–154

Contents lists available at SciVerse ScienceDirect

Journal of Cardiology

journal homepage: www.elsevier.com/locate/jjcc

Original article

A comparison between 40 MHz intravascular ultrasound iMap imaging system and integrated backscatter intravascular ultrasound

Ryotaro Yamada (MD), Hiroyuki Okura (MD, FJCC)*, Teruyoshi Kume (MD), Yoji Neishi (MD), Takahiro Kawamoto (MD), Yoshinori Miyamoto (MD), Koichiro Imai (MD), Ken Saito (MD), Akihiro Hayashida (MD), Kiyoshi Yoshida (MD, FJCC)

Department of Cardiology, Kawasaki Medical School, Kurashiki, Japan

ARTICLE INFO

Article history:
Received 26 June 2012
Received in revised form
23 September 2012
Accepted 28 October 2012
Available online 21 December 2012

Keywords:
Intravascular ultrasound
Atherosclerosis
Coronary artery disease

ABSTRACT

Background: iMap is a newly developed intravascular ultrasound (IVUS) tissue characterization system based on pattern recognition of the radio frequency (RF) signals.
Purpose: The purpose of this study was to compare tissue characterization between iMap and another previously validated tissue characterization system, integrated backscatter (IB)-IVUS in vivo and to clarify similarities and differences between these two methods.
Methods: A total of 31 lesions from 16 patients with ischemic heart disease were studied. IVUS imaging was performed using 40 MHz IVUS catheter. RF signals from each lesion were then exported to analyze tissue characterization using both iMap and IB-IVUS. By iMap, coronary plaque was classified into four categories, fibrotic, lipidic, necrotic, or calcified. By IB-IVUS, coronary plaque was classified into four categories, fibrosis, lipid pool, dense fibrosis, or calcification. After the images were acquired, IB-IVUS and iMap images were compared at exactly the same cross-sections. Because severe calcification is a perfect reflector, dense calcification lesions (>20%) were excluded.
Results: Both fibrotic and calcified by iMap correlated well with fibrosis and calcification by IB-IVUS (fibrotic vs. fibrosis: $r^2 = 0.522$, $p < 0.001$, calcified vs. calcification: $r^2 = 0.560$, $p < 0.001$). Although lipidic by iMap did not correlate with lipid pool by IB-IVUS, necrotic by iMap correlated well with lipid pool by IB-IVUS ($r^2 = 0.480$, $p < 0.001$).
Conclusion: Although tissue types classified by iMap correlated well with corresponding tissue type by IB-IVUS, some discrepancy presented between the two systems. These results may call for careful interpretation of the tissue types obtained by the different IVUS tissue characterization systems.

Introduction

Intravascular ultrasound (IVUS) is widely used for evaluating vascular wall structure of the coronary artery in the clinical setting [1]. Previous studies have demonstrated that plaque rupture may lead to thrombus formation and acute coronary syndrome (ACS) [2–4]. Pathological and IVUS studies have suggested that presence of necrotic core and overlying thin fibrous cap as well as presence of positive remodeling are morphological findings of unstable or vulnerable plaque [5,6]. Although conventional gray scale IVUS predicts presence of positive remodeling, objective and quantitative plaque assessments have not been possible [7–16].

Recently, the integrated backscatter (IB)-IVUS system (YD Co, Ltd, Nara, Japan), which provides two-dimensional color-coded maps for the tissue characterization of coronary plaques, has been developed and become commercially available. A good correlation was reported between plaque characteristics obtained by IB-IVUS and histological findings [17]. Furthermore, it has been reported that IB-IVUS may be useful to detect thin-cap fibroatheroma (TCFA) [18] and predict future acute coronary syndrome [19].

iMap (Boston Scientific, MA, USA) is another newly developed IVUS tissue characterization system based on pattern recognition of the radio frequency (RF) signals [20–23]. Because IB-IVUS and iMap use different algorithms, it is possible that there may be differences in tissue characterization of the coronary plaque.

Therefore, the purpose of this study was to compare tissue characterization between iMap and IB-IVUS in vivo and to clarify similarities and differences between these two methods.

DOI of commentary article: http://dx.doi.org/10.1016/j.jjcc.2013.01.001.
* Corresponding author at: Department of Cardiology, Kawasaki Medical School, 577 Matsushima, Kurashiki, 701-0192, Japan. Tel.: +81 86 462 1111; fax: +81 86 464 4060.
E-mail address: hokura@fides.dti.ne.jp (H. Okura).

0914-5087/$ – see front matter
http://dx.doi.org/10.1016/j.jjcc.2012.10.008

Methods

Study population

A total of 16 patients (12 males, 4 females, age 65 ± 12 years) with ischemic heart disease who underwent coronary stent implantation under IVUS guidance were enrolled in this study. Patients with acute myocardial infarction, thrombotic lesion, restenotic lesion, chronic total occlusion, severe valvular disease, cardiogenic shock or unstable hemodynamics, renal failure, unsuitable coronary artery anatomy for IVUS examination, and inaccessible quality of IVUS imaging were excluded.

Written informed consent was obtained from all patients before cardiac catheterization and IVUS examinations.

Thirty-one segments were selected based on the outcomes from angiography as follows: angiographic diameter stenosis between 75% and 90%.

IVUS imaging was performed using a commercially available 40 MHz IVUS catheter (Atlantis Pro2, Boston Scientific, Natick, MA, USA) with an automatic pullback device at 0.5 mm/s before percutaneous coronary intervention (PCI).

RF signals from each segment were then used to analyze tissue characterization using both iMap and IB-IVUS.

The data were digitized for quantitative and qualitative analysis according to the criteria of the American College of Cardiology Clinical Expert Consensus document on IVUS [24]. Thirty-one external elastic membrane (EEM) and lumen cross-sectional area (CSA) samples were traced and measured. Plaque plus media (P + M) CSA was calculated by EEM-lumen CSA. Percent plaque burden was calculated by (P + M CSA/EEM CSA) × 100. Interobserver variability for EEM CSA and lumen CSA were 4.6 ± 3.0% and 6.5 ± 3.3%, respectively. Intraobserver variability for EEM CSA and lumen CSA were 4.0 ± 2.9% and 4.5 ± 2.7%, respectively.

iMap

To obtain iMap images, the system was connected to an imaging system (iLab, Boston Scientific), signal trigger output, and video image output to obtain the RF signal. Ultrasound backscattered signals were acquired using an Atlantis pro2, digitized, and subjected to spectral analysis. The IB values for each tissue component were expressed in decibels (dB) and calculated using a fast-Fourier transform of the frequency component of the backscattered signal from a small volume of tissue. Conventional IVUS images and color-coded maps were displayed side-by-side on a monitor. The EEM and lumen were then semi-automatically traced. By iMap, coronary plaque was classified into four categories, fibrotic (green), lipidic (yellow), necrotic (pink), or calcified (blue). Furthermore, iMap provides the confidence level based on the degree of spectrum algorithm characteristics similarity assessed from previous analysis of different cadaver hearts.

IB-IVUS

To obtain IB-IVUS images, a commercially available image processing system (YD Co, Ltd) was connected to an imaging system (Galaxy, Boston Scientific) with RF output, signal trigger output, and video image output to obtain the RF signal. Ultrasound backscattered signals were acquired using a 40-MHz mechanically-rotating IVUS catheter (Atlantis pro2), digitized and subjected to spectral analysis. The IB values for each tissue component were expressed in dB and calculated using a fast-Fourier transform of the frequency component of the backscattered signal from a small volume of tissue. Conventional IVUS images and color-coded maps were displayed side-by-side on a monitor. We excluded the vessel lumen and area outside of the internal elastic membrane from the color-coded maps by manually tracing the vessel lumen and internal elastic membrane on the conventional IVUS images. By IB-IVUS, coronary plaque was classified into four categories, fibrosis (green), dense fibrosis (yellow), lipid pool (blue), and calcification (red).

After the images were acquired, IB-IVUS and iMap images were compared at exactly the same cross-sectional image. Because severe calcification is a perfect reflector, dense calcification lesions (>20%) were excluded. The identical cross-section for analysis was carefully selected using intravascular or perivascular landmarks and a constant pullback speed [18,25].

Statistics

Statistical analysis was performed with StatView version 5.0 (SAS Institute, Cary, NC, USA). Qualitative data are presented with frequencies, and quantitative data are shown as mean ± SD, if indicated. Continuous variables are reported as mean ± SD. Paired t tests were used to differentiate two sets of data with normal distribution. Wilcoxon signed rank test was performed when the data were not normally distributed. The association between IB-IVUS and iMap indices was investigated with two different analyses: (1) linear regression and (2) Bland–Altman analysis of agreement. The latter analysis was used to compare the mean difference and SD between the values from IB-IVUS and iMap. In these analyses, a value of $p < 0.05$ was considered to be significant.

Results

Baseline and procedural characteristics

An IVUS catheter was positioned beyond the target lesions in all enrolled cases. The target vessel was the left anterior descending artery in 13 (42%), circumflex artery in 10 (32%), and right coronary artery in 8 (26%). Patients' characteristics are shown in Table 1.

Qualitative parameters and tissue characterization of IB-IVUS and iMap

Representative cross-sectional images obtained by using IB-IVUS and iMap are shown in Fig. 1. Table 2 shows qualitative parameters and tissue characterization of IB-IVUS and iMap. There were no significant differences in EEM-CSA, lumen CSA, P + M CSA and plaque burden between IB-IVUS and iMap. Confidence level of each tissue characterization is also shown in Table 2.

Table 1
Patient characteristics.

Characteristics	Value
Sample size	16
Age, years	65 ± 12
Male sex	12 (75%)
Body Mass Index	24 ± 4
Vessels	
LAD	13 (42%)
LCX	10 (32%)
RCA	8 (26%)
Conditions	
Hypertension	11 (69%)
Hyperlipidemia	10 (63%)
Diabetes mellitus	7 (44%)
Smoking	8 (50%)
Family history	4 (25%)
Dx stable angina pectoris	12 (75%)
Unstable angina pectoris	4 (25%)

Data are presented as no. (%) or mean ± SD, unless otherwise indicated. LAD, left anterior descending artery; LCX, left circumflex artery; RCA, right coronary artery.

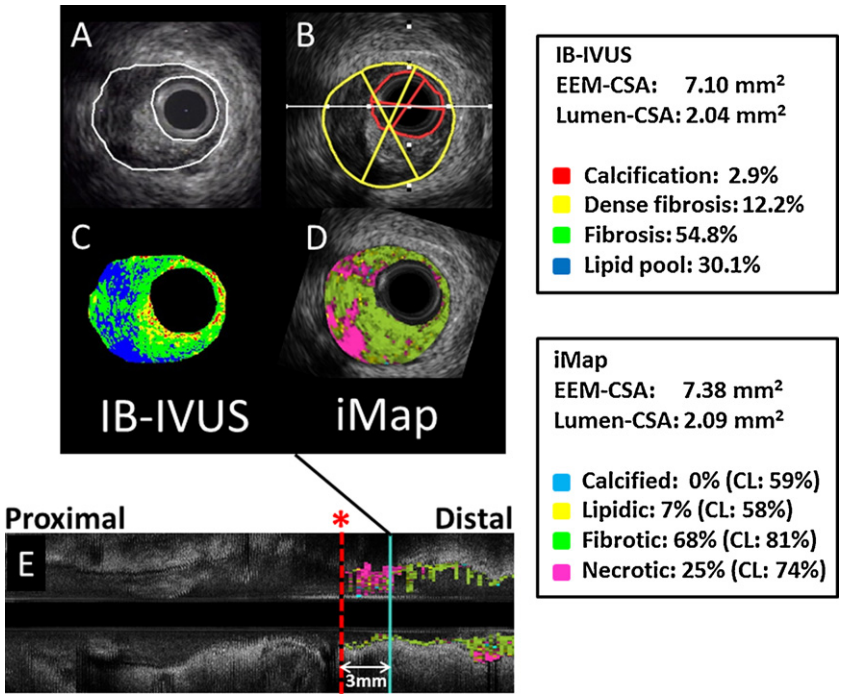

Fig. 1. Representative images obtained by using integrated backscatter-intravascular ultrasound (IB-IVUS) and iMap. Both IVUS images were carefully selected at 3 mm distal from the branch (*) and compared. The images shown are as follows: (A) gray scale image (IB-IVUS); (B) gray scale image (iMap); (C) color-coded image (IB-IVUS); (D) color-coded image (iMap); (E) longitudinally reconstructed IVUS image. EEM, external elastic membrane; CSA, cross-sectional area. (For interpretation of the references to color in this figure legend, the reader is referred to the web version of this article.)

Table 2
Qualitative parameters and tissue characterization.

	IB-IVUS	iMap (Confidence level, %)		p
EEM-CSA, mm²	11.6 ± 4.2	11.3 ± 3.9		0.793
Lumen CSA, mm²	3.4 ± 1.7	3.6 ± 1.7		0.741
P + M CSA, mm²	8.2 ± 3.4	7.8 ± 3.0		0.612
Plaque burden, %	70.2 ± 9.5	68.5 ± 9.6		0.481
IB-IVUS				
Calcification, %	3.4 ± 2.9			-
Dense fibrosis , %	7.5 ± 3.6			-
Fibrosis, %	48.5 ± 13.9			-
Lipid pool, %	40.6 ± 16.7			-
iMap				
Calcified, %		3.6 ± 3.7	(70.6 ± 17.2 %)	-
Lipidic, %		6.2 ± 2.5	(58.7 ± 2.5 %)	-
Fibrotic, %		57.8 ± 17.5	(79.4 ± 4.2 %)	-
Necrotic, %		32.5 ± 16.0	(76.5 ± 9.4 %)	-

Correlation between IB-IVUS and iMap

Both fibrotic and calcified by iMap correlated well with fibrosis and calcification by IB-IVUS (fibrotic vs. fibrosis: $r^2 = 0.522$, $p < 0.001$; calcified vs. calcification: $r^2 = 0.560$, $p < 0.001$) (Figs. 2 and 3). A Bland–Altman test showed good agreement of the value of both indices between iMap and IB-IVUS.

Although lipidic by iMap did not correlate with lipid pool by IB-IVUS ($r^2 = 0.071$, $p = 0.149$), necrotic by iMap correlated well with lipid pool by IB-IVUS ($r^2 = 0.480$, $p < 0.001$). A Bland–Altman test showed good agreement between necrotic and lipid pool (Fig. 4).

Discussion

The primary findings of our present study were: 1) fibrosis and calcification by IB-IVUS correlated well with corresponding tissue type, fibrotic and calcified by iMap; however, 2) lipid pool by IB-IVUS did not correlate with lipidic by iMap, but correlated well with necrotic by iMap.

Recently, three different IVUS tissue characterization systems, virtual histology (VH)-IVUS (Volcano Therapeutics, Inc., Rancho Cordova, CA, USA), IB-IVUS, and iMap, have become commercially available. Although all of these IVUS systems have defined their

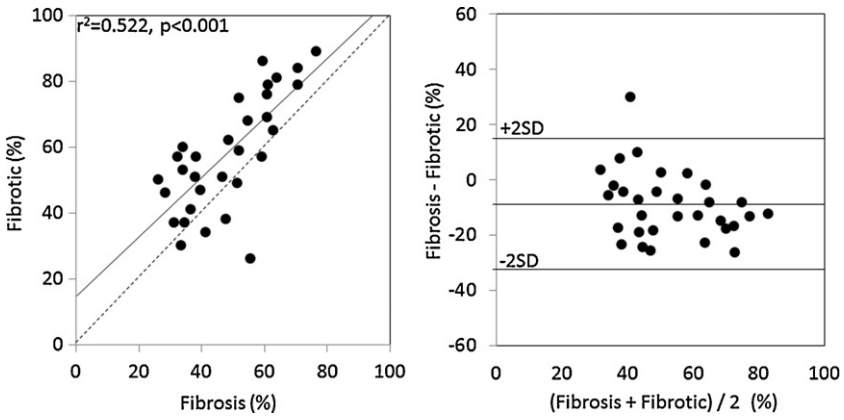

Fig. 2. Correlation between fibrotic by iMap and fibrosis by integrated backscatter-intravascular ultrasound (IB-IVUS) (left). Bland–Altman test for fibrotic and fibrosis (right). Fibrotic by iMap correlated well with fibrosis by IB-IVUS ($r^2 = 0.522$, $p < 0.001$).

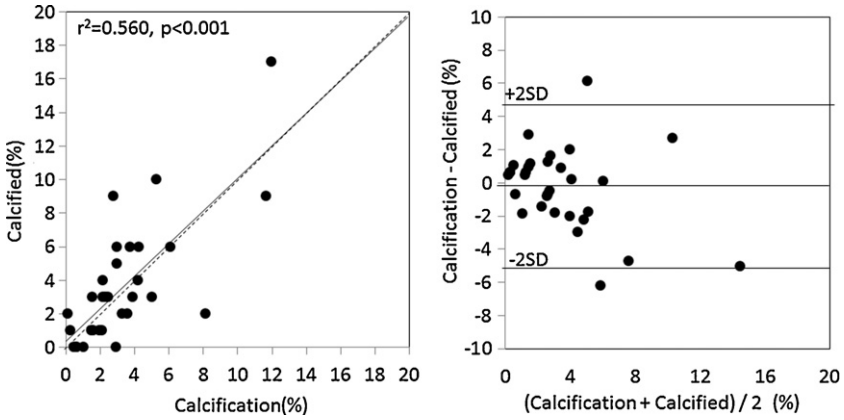

Fig. 3. Correlation between calcified by iMap and calcification by integrated backscatter-intravascular ultrasound (IB-IVUS) (left). Bland–Altman test for calcified and calcification (right). Calcified by iMap correlated well with calcification by IB-IVUS ($r^2 = 0.560$, $p < 0.001$).

own tissue types based on ex vivo and/or in vivo validation with histopathology, the relationship between tissue types of different tissue characterization systems have not been well conducted [20,26–29]. Our results showing that fibrous plaque (named as fibrosis by IB-IVUS and fibrotic by iMap) and calcified plaque (named as calcification by IB-IVUS and calcified by iMap) were similarly detected and quantified by both systems have an important clinical implication. These two different IVUS tissue characterization systems may be used alternatively to each other when assessing amount of fibrous and calcified tissue.

On the other hand, despite the similar name used by each system, lipid pool by IB-IVUS did not correlate with lipidic by iMap. This also has an important clinical implication. A previous study demonstrated that atheroma has various components such as micro-calcification in addition to the lipid pool [30]. Furthermore, Hara et al. found a significant increase of IB variance in the axial direction along with the accumulation of intraplaque lipids [31]. Heterogeneity of plaque composition and the distance from a transducer to regions of interest may lead to larger IB difference and different tissue characterization. In our study, confidence levels

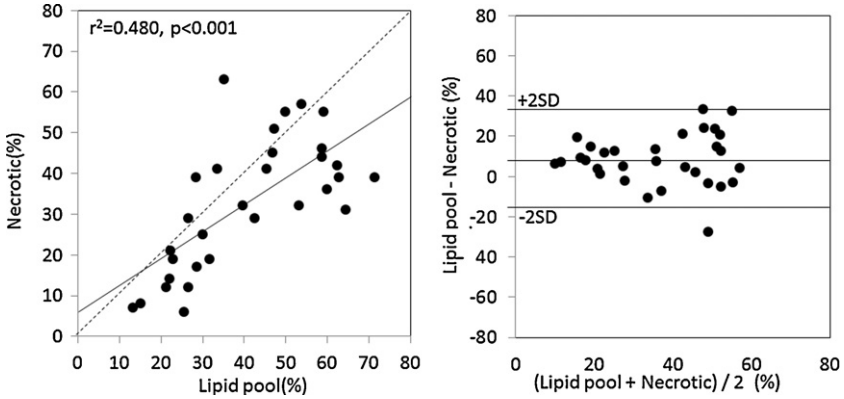

Fig. 4. Correlation between necrotic by iMap and lipid pool by integrated backscatter-intravascular ultrasound (IB-IVUS) (left). Bland–Altman test for necrotic and lipid pool (right). Necrotic by iMap correlated well with lipid pool by IB-IVUS ($r^2 = 0.480$, $p < 0.001$).

of fibrotic, calcific, and necrotic were obviously higher than lipidic. Similarly, those findings might be affected by various components in lipid pool.

Other studies have shown that the amount of lipid pool by IB-IVUS is related to myonecrosis during PCI possibly because of distal embolization [32]. Furthermore, another study by Sano et al. has demonstrated the lipid pool by IB-IVUS is related to future ACS events [19]. More recently, Miyamoto et al. have demonstrated that the amount of lipid pool is significantly larger in TCFA (defined by optical coherence tomography; OCT) and therefore, IB-IVUS may be useful in detecting TCFA by OCT [18]. Because lipidic by iMap did not correlate with lipid pool by IB-IVUS, it is unclear if lipidic by iMap predicts distal embolization during PCI or future ACS events. On the other hand, necrotic by iMap may predict distal embolization during PCI and future ACS events considering its similarity to lipid pool by IB-IVUS.

Several studies have shown that VH-IVUS may be useful in detecting distal embolization or slow flow/no reflow during PCI [33–35]. More recently, a prospective, multicenter study, PROSPECT (Providing Regional Observations to Study Predictors of Events in the Coronary Tree) trial demonstrated that VH-IVUS derived TCFA was one of the strongest independent predictors of untreated, non-culprit lesion-related events [36]. Because our present study did not compare VH-IVUS and iMap, it is still unknown whether necrotic core by VH-IVUS correlates with necrotic by iMap.

Study limitations

Firstly, this is a study with small numbers from a single center experience. Thus the results need to be confirmed by a larger multicenter study.

Secondly, all current commercially available IVUS tissue characterization software packages have a similar limitation in which they cannot show tissue components behind a severe calcification and guidewire. Calcium and guidewires lead to acoustic shadowing which could mislead the RF signal-based tissue characterization. To take into account those acoustic shadow areas, dense calcification lesions were excluded in this study. Therefore, there might be some bias in the result.

Thirdly, although we compared in vivo IVUS-derived tissue characterization using two different systems, direct comparison between IVUS-tissue characterization and histology was not performed. Therefore, it is inconclusive which tissue characterization correlates better with histological findings. Further study will be needed to compare three different IVUS tissue characterizations and histology.

Conclusions

Although some tissue types classified by iMap correlated well with corresponding tissue type by IB-IVUS, others did not. These results may call for careful interpretation of the tissue types obtained by the different IVUS tissue characterization systems.

Conflict of interest

All authors have no conflict of interest or financial disclosure regarding this manuscript.

References

[1] Nissen SE, Yock P. Intravascular ultrasound: novel pathophysiological insights and current clinical applications. Circulation 2001;103:604–16.
[2] Davies MJ, Richardson PD, Woolf N, Katz DR, Mann J. Risk of thrombosis in human atherosclerotic plaques: role of extracellular lipid, macrophage, and smooth muscle cell content. Br Heart J 1993;69:377–81.
[3] Felton CV, Crook D, Davies MJ, Oliver MF. Relation of plaque lipid composition and morphology to the stability of human aortic plaques. Arterioscler Thromb Vasc Biol 1997;17:1337–45.
[4] Yabushita H, Bouma BE, Houser SL, Aretz HT, Jang IK, Schlendorf KH, Kauffman CR, Shishkov M, Kang DH, Halpern EF, Tearney GJ. Characterization of human atherosclerosis by optical coherence tomography. Circulation 2002;106:1640–5.
[5] Kotani J, Mintz GS, Rai PB, Pappas CK, Gevorkian N, Bui AB, Pichard AD, Satler LF, Suddath WO, Waksman R, Laird Jr JR, Kent KM, Weissman NJ. Intravascular ultrasound assessment of angiographic filling defects in native coronary arteries: do they always contain thrombi? J Am Coll Cardiol 2004;44:2087–9.
[6] Virmani R, Burke AP, Farb A, Kolodgie FD. Pathology of the vulnerable plaque. J Am Coll Cardiol 2006;47:C13–8.
[7] Dangas G, Mintz GS, Mehran R, Lansky AJ, Kornowski R, Pichard AD, Satler LF, Kent KM, Stone GW, Leon MB. Preintervention arterial remodeling as an independent predictor of target-lesion revascularization after nonstent coronary intervention: an analysis of 777 lesions with intravascular ultrasound imaging. Circulation 1999;99:3149–54.
[8] Glagov S, Weisenberg E, Zarins CK, Stankunavicius R, Kolettis GJ. Compensatory enlargement of human atherosclerotic coronary arteries. N Engl J Med 1987;316:1371–5.
[9] Hibi K, Ward MR, Honda Y, Suzuki T, Jeremias A, Okura H, Hassan AH, Maehara A, Yeung AC, Pasterkamp G, Fitzgerald PJ, Yock PG. Impact of different definitions on the interpretation of coronary remodeling determined by intravascular ultrasound. Catheter Cardiovasc Interv 2005;65:233–9.
[10] Kaji S, Akasaka T, Hozumi T, Takagi T, Kawamoto T, Ueda Y, Yoshida K. Compensatory enlargement of the coronary artery in acute myocardial infarction. Am J Cardiol 2000;85:1139–41. A9.
[11] Nakamura M, Nishikawa H, Mukai S, Setsuda M, Nakajima K, Tamada H, Suzuki H, Ohnishi T, Kakuta Y, Nakano T, Yeung AC. Impact of coronary artery remodeling on clinical presentation of coronary artery disease: an intravascular ultrasound study. J Am Coll Cardiol 2001;37:63–9.
[12] Nishioka T, Luo H, Eigler NL, Berglund H, Kim CJ, Siegel RJ. Contribution of inadequate compensatory enlargement to development of human coronary artery stenosis: an in vivo intravascular ultrasound study. J Am Coll Cardiol 1996;27:1571–6.
[13] Okura H, Hayase M, Shimodozono S, Bonneau HN, Yock PG, Fitzgerald PJ. Impact of pre-interventional arterial remodeling on subsequent vessel behavior after balloon angioplasty: a serial intravascular ultrasound study. J Am Coll Cardiol 2001;38:2001–5.
[14] Okura H, Morino Y, Oshima A, Hayase M, Ward MR, Popma JJ, Kuntz RE, Bonneau HN, Yock PG, Fitzgerald PJ. Preintervention arterial remodeling affects clinical outcome following stenting: an intravascular ultrasound study. J Am Coll Cardiol 2001;37:1031–5.
[15] Okura H, Taguchi H, Kubo T, Toda I, Yoshiyama M, Yoshikawa J, Yoshida K. Impact of arterial remodelling and plaque rupture on target and non-target lesion revascularisation after stent implantation in patients with acute coronary syndrome: an intravascular ultrasound study. Heart 2007;93:1219–25.
[16] Schoenhagen P, Ziada KM, Kapadia SR, Crowe TD, Nissen SE, Tuzcu EM. Extent and direction of arterial remodeling in stable versus unstable coronary syndromes: an intravascular ultrasound study. Circulation 2000;101:598–603.
[17] Okubo M, Kawasaki M, Ishihara Y, Takeyama U, Kubota T, Yamaki T, Ojio S, Nishigaki K, Takemura G, Saio M, Takami T, Minatoguchi S, Fujiwara H. Development of integrated backscatter intravascular ultrasound for tissue characterization of coronary plaques. Ultrasound Med Biol 2008;34:655–63.
[18] Miyamoto Y, Okura H, Kume T, Kawamoto T, Neishi Y, Hayashida A, Yamada R, Imai K, Saito K, Yoshida K. Plaque characteristics of thin-cap fibroatheroma evaluated by OCT and IVUS. JACC Cardiovasc Imaging 2011;4:638–46.
[19] Sano K, Kawasaki M, Ishihara Y, Okubo M, Tsuchiya K, Nishigaki K, Zhou X, Minatoguchi S, Fujita H, Fujiwara H. Assessment of vulnerable plaques causing acute coronary syndrome using integrated backscatter intravascular ultrasound. J Am Coll Cardiol 2006;47:734–41.
[20] Sathyanarayana S, Carlier S, Li W, Thomas L. Characterisation of atherosclerotic plaque by spectral similarity of radiofrequency intravascular ultrasound signals. EuroIntervention 2009;5:133–9.
[21] Garcia-Garcia HM, Costa MA, Serruys PW. Imaging of coronary atherosclerosis: intravascular ultrasound. Eur Heart J 2010;31:2456–69.
[22] Utsunomiya M, Hara H, Moroi M, Sugi K, Nakamura M. Relationship between tissue characterization with 40 MHz intravascular ultrasound imaging and 64-slice computed tomography. J Cardiol 2011;57:297–302 [Comparative Study].
[23] Araki T, Nakamura M, Utsunomiya M, Sugi K. Visualization of coronary plaque in type 2 diabetes mellitus patients using a new 40 MHz intravascular ultrasound imaging system. J Cardiol 2012;59:42–9.
[24] Mintz GS, Nissen SE, Anderson WD, Bailey SR, Erbel R, Fitzgerald PJ, Pinto FJ, Rosenfield K, Siegel RJ, Tuzcu EM, Yock PG. American College of Cardiology Clinical Expert Consensus Document on Standards for Acquisition, Measurement and Reporting of Intravascular Ultrasound Studies (IVUS). A report of the American College of Cardiology Task Force on Clinical Expert Consensus Documents. J Am Coll Cardiol 2001;37:1478–92.
[25] Yamada R, Okura H, Kume T, Saito K, Miyamoto Y, Imai K, Tsuchiya T, Maehama T, Okahashi N, Obase K, Hayashida A, Neishi Y, Kawamoto T, Yoshida K. Relationship between arterial and fibrous cap remodeling: a serial three-vessel intravascular ultrasound and optical coherence tomography study. Circ Cardiovasc Interv 2010;3:484–90.
[26] Kawasaki M, Takatsu H, Noda T, Sano K, Ito Y, Hayakawa K, Tsuchiya K, Arai M, Nishigaki K, Takemura G, Minatoguchi S, Fujiwara T, Fujiwara H. In vivo

quantitative tissue characterization of human coronary arterial plaques by use of integrated backscatter intravascular ultrasound and comparison with angioscopic findings. Circulation 2002;105:2487–92.
[27] Nasu K, Tsuchikane E, Katoh O, Vince DG, Virmani R, Surmely JF, Murata A, Takeda Y, Ito T, Ehara M, Matsubara T, Terashima M, Suzuki T. Accuracy of in vivo coronary plaque morphology assessment: a validation study of in vivo virtual histology compared with in vitro histopathology. J Am Coll Cardiol 2006;47:2405–12.
[28] Okubo M, Kawasaki M, Ishihara Y, Takeyama U, Yasuda S, Kubota T, Tanaka S, Yamaki T, Ojio S, Nishigaki K, Takemura G, Saio M, Takami T, Fujiwara H, Minatoguchi S. Tissue characterization of coronary plaques: comparison of integrated backscatter intravascular ultrasound with virtual histology intravascular ultrasound. Circ J 2008;72:1631–9.
[29] Garcia-Garcia HM, Gogas BD, Serruys PW, Bruining N. IVUS-based imaging modalities for tissue characterization: similarities and differences. Int J Cardiovasc Imaging 2011;27:215–24.
[30] Virmani R, Kolodgie FD, Burke AP, Farb A, Schwartz SM. Lessons from sudden coronary death: a comprehensive morphological classification scheme for atherosclerotic lesions. Arterioscler Thromb Vasc Biol 2000;20:1262–75.
[31] Hara H, Tsunoda T, Nemoto N, Yokouchi I, Yamamoto M, Ono T, Moroi M, Suzuki M, Sugi K, Nakamura M. Distribution of ultrasonic radiofrequency signal amplitude detects lipids in atherosclerotic plaque of coronary arteries: an ex-vivo study. Cardiovasc Ultrasound 2008;6:18.
[32] Uetani T, Amano T, Ando H, Yokoi K, Arai K, Kato M, Marui N, Nanki M, Matsubara T, Ishii H, Izawa H, Murohara T. The correlation between lipid volume in the target lesion, measured by integrated backscatter intravascular ultrasound, and post-procedural myocardial infarction in patients with elective stent implantation. Eur Heart J 2008;29:1714–20.
[33] Kawamoto T, Okura H, Koyama Y, Toda I, Taguchi H, Tamita K, Yamamuro A, Yoshimura Y, Neishi Y, Toyota E, Yoshida K. The relationship between coronary plaque characteristics and small embolic particles during coronary stent implantation. J Am Coll Cardiol 2007;50:1635–40.
[34] Hong YJ, Jeong MH, Choi YH, Ko JS, Lee MG, Kang WY, Lee SE, Kim SH, Park KH, Sim DS, Yoon NS, Youn HJ, Kim KH, Park HW, Kim JH, et al. Impact of plaque components on no-reflow phenomenon after stent deployment in patients with acute coronary syndrome: a virtual histology-intravascular ultrasound analysis. Eur Heart J 2011;32:2059–66.
[35] Hong YJ, Mintz GS, Kim SW, Lee SY, Okabe T, Pichard AD, Satler LF, Waksman R, Kent KM, Suddath WO, Weissman NJ. Impact of plaque composition on cardiac troponin elevation after percutaneous coronary intervention: an ultrasound analysis. JACC Cardiovasc Imaging 2009;2:458–68.
[36] Stone GW, Maehara A, Lansky AJ, de Bruyne B, Cristea E, Mintz GS, Mehran R, McPherson J, Farhat N, Marso SP, Parise H, Templin B, White R, Zhang Z, Serruys PW. A prospective natural-history study of coronary atherosclerosis. N Engl J Med 2011;364:226–35.